Supporting information (SI)

# DNA Structural Alteration Leading to Antibacterial Properties of 6-Nitroquinoxaline Derivatives

Khondakar Sayef Ahammed,[†,§] Ritesh Pal,[†, ‡,§] Jeet Chakraborty,[†,§] Ajay Kanungo,[†, ‡] Polnati Sravani Purnima,[†] Sanjay Dutta *[, †, ‡]

† Organic and Medicinal Chemistry Division, CSIR- Indian Institute of Chemical Biology

4, Raja S.C. Mullick Road, Kolkata-700032, West Bengal, India.

E-mail: sanjaydutta@iicb.res.in

‡ Academy of Scientific and Innovative Research (AcSIR), Kolkata-700032, West Bengal, India.

§These authors contributed equally.

* Corresponding author.

## Table of Contents

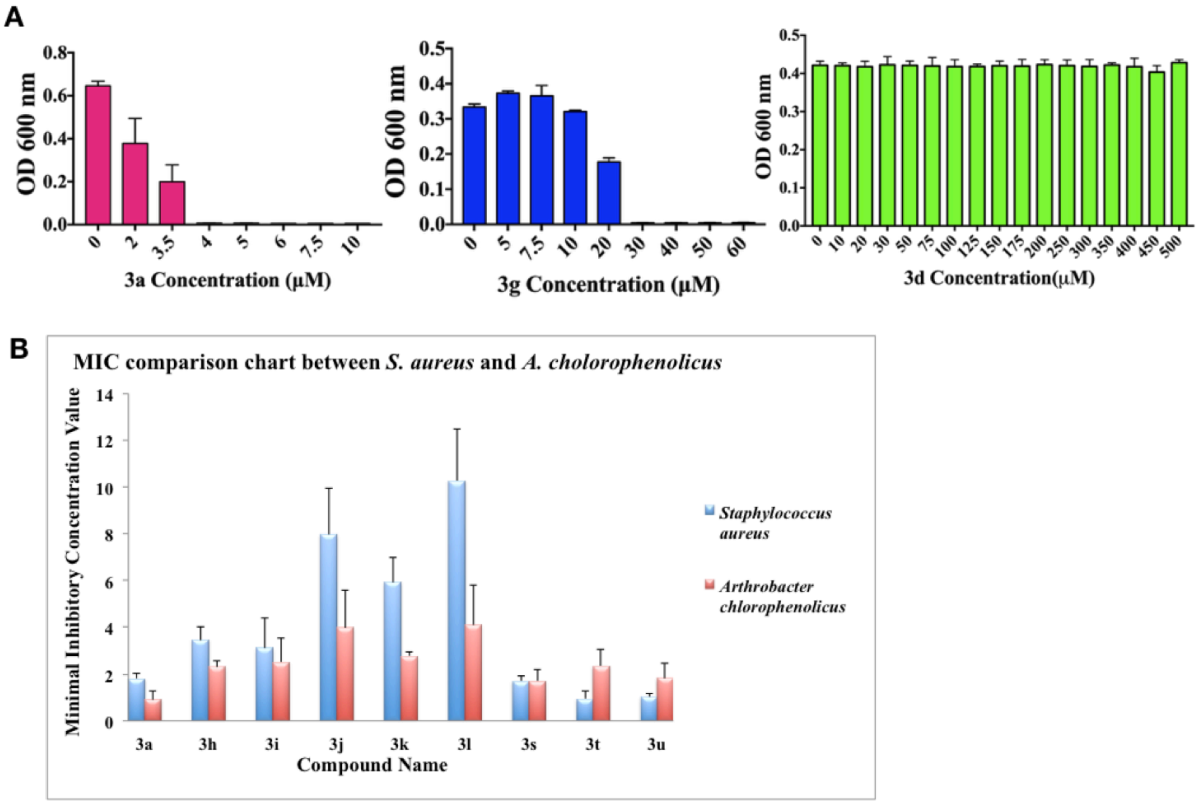


**Supporting Figure S1:**(A) MIC values of *S. aureus* cells treated with indicated compounds (**3a**, **3g**, **3d**) and incubated for 6 h at 37 $^{o}$C.[1, 2] (B) Comparison of MIC values of para substituted derivatives (**3a**, **3h**, **3i, 3j, 3k, 3l**) and disubstituted derivatives (**3s**, **3t**, **3u**) between *S. aureus* and *A. chlorophenolicus*.

**Time-kill assay:**

Monitoring the rate of bacteriocidal or bacteriostatic activity in the presence of varying concentrations of the antimicrobial compounds is very crucial in determining the actual effect of the drug against a growing population of the bacterial cells.[3] In this study, the growth kinetics of *S. aureus* cells in the presence of designed compounds were evaluated by an *in-vitro* time-kill assay. Log phase *S. aureus* cells (3 x $10^5$ cells/mL) were treated with **3a**, **3d**, **3u**, **3q** and kananycin (as a positive control), incubated at 37 °C and OD was measured (at 600 nm) at 1.5 hours interval. Results indicate that the compounds **3a**, **3q** and **3u** were able to inhibit the growth of the bacterial cell at double-MIC concentrations while **3d** was unable to inhibit the growth of the cells (Figure S2).

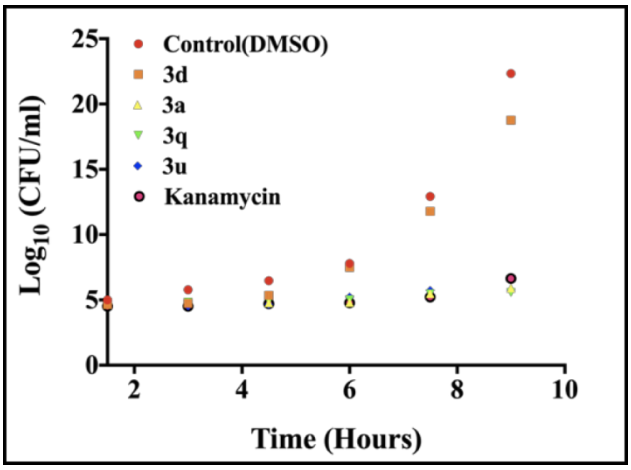


**Supporting Figure S2:** Time−kill kinetic study of the compounds (**3a**, **3d**, **3q**, **3u** and kanamycin) against *S. aureus*. $3x10^5$ cells were inoculated, treated with DMSO (0.5 %) or indicated compounds. Log CFU/mL was plotted against different time (hour).

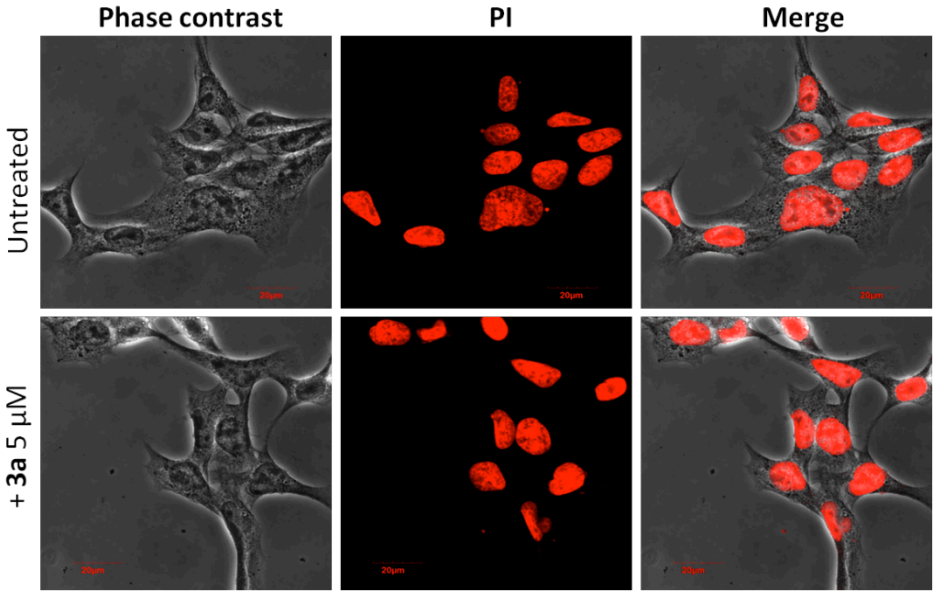


**Supporting Figure S3:** Cellular morphology of HEK 293 cells, untreated or treated with **3a**, stained with propidium iodide (PI, nuclear stain) cells were visualized in 60x magnification. Scale bar- 20 µm.[3]

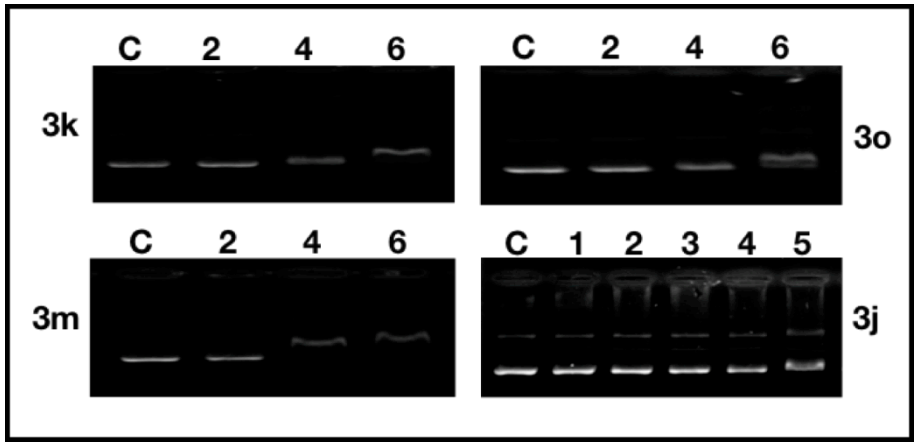


**Supporting Figure S4:** Agarose gel shift assay with **3k, 3o, 3m** and **3j**. Lane number indicates [compound]/[DNA base pair] ratios.[4]

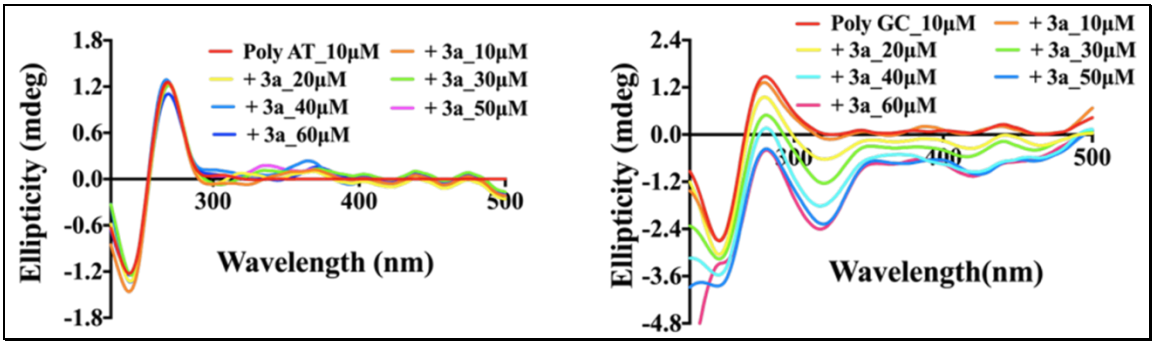


**Supporting Figure S5:** Circular dichroism (CD) spectra of 10 μM poly-AT DNA (left) and poly-GC DNA (right) titrated with **3a** in an increasing concentrations from 10 to 60 μM.[4]

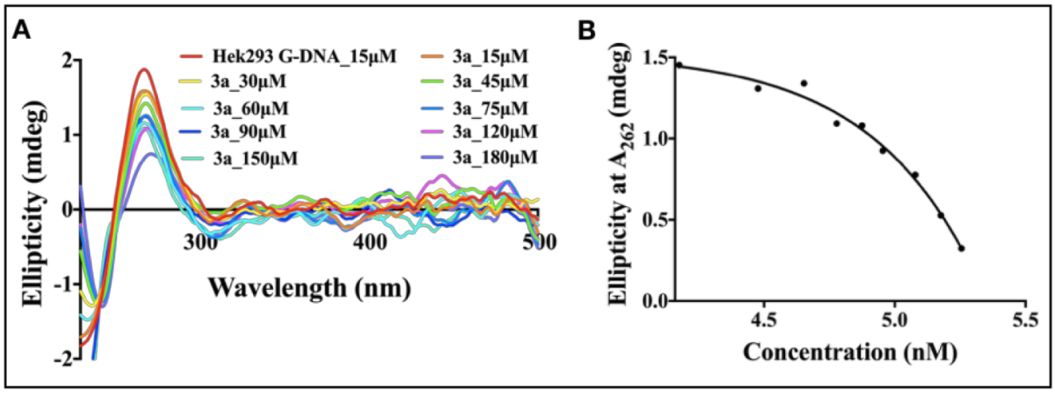


**Supporting Figure S6:** (A) Circular dichroism (CD) spectra of 15 μM mammalian genomic DNA (isolated from HEK 293 cell line) titrated with **3a** in an increasing concentrations of 15, 30, 45, 60, 75, 90, 120, 150,180 μM. (B) Ellipticity plot at 262 nm bands of CD spectra.

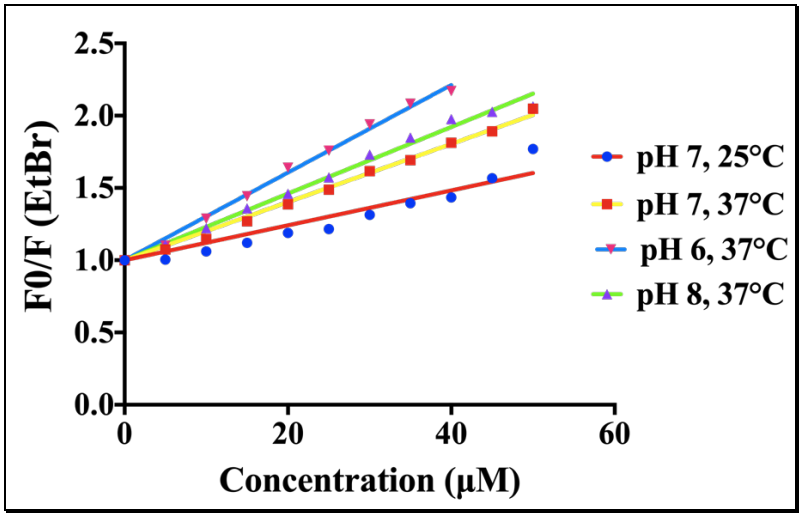


**Supporting Figure S7:** Quenching plot of fluorescence intercalator displacement assay (FID) with 10 µM *S. aureus* genomic DNA and 5 µM EtBr ($\lambda_{ex}$ = 480 nm) titrated with **3a** (2.5-50 µM) at indicated pH and temperature. $K_{SV}$ values at (pH 8, 37 °C is 2.3 x $10^4$ $M^{-1}$, pH 7, 37 °C is 2.0 x $10^4$ $M^{-1}$, pH 6, 37 °C is 3.0 x $10^4$ $M^{-1}$).

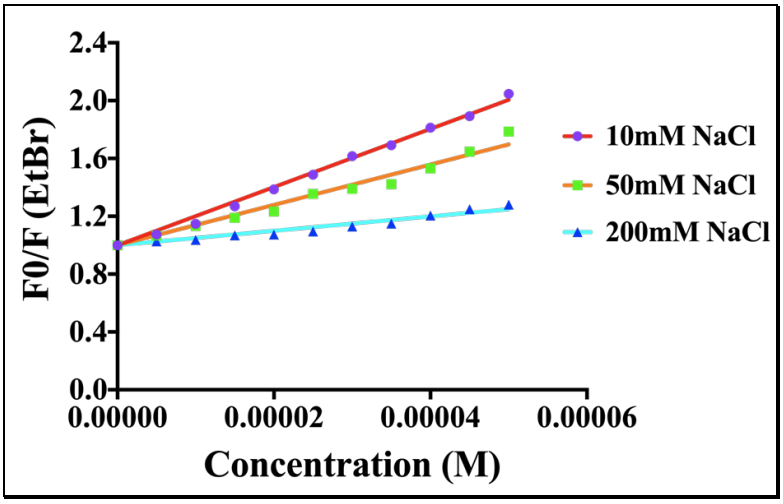


**Supporting Figure S8:** Quenching plot of fluorescence intercalator displacement assay (FID) with 10 µM *S. aureus* genomic DNA and 5 µM EtBr ($\lambda_{ex}$ = 480 nm) with indicated salt concentration.

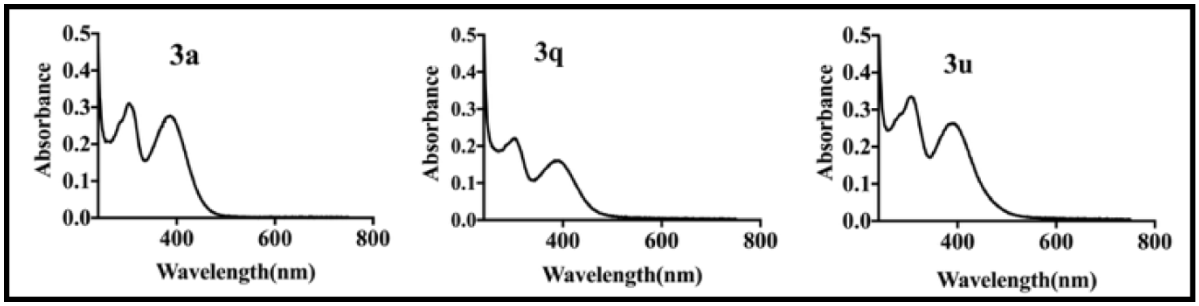


**Supporting Figure S9:** UV absorption spectra of compounds **3a**, **3q**, **3u** in 10 mM phosphate buffer at pH 7.0 with 10 mM NaCl and 1 % DMSO at $25^0$ C.

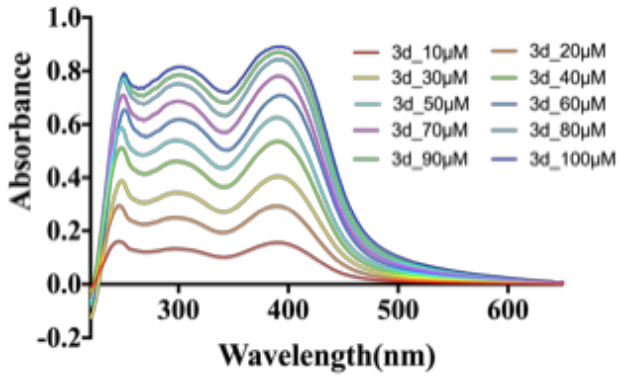


**Supporting Figure S10:** UV absorption spectra of compound **3d** (in 10 mM phosphate buffer at pH 7.0 with 10 mM NaCl and 1 % DMSO at $25^0$ C) with an increasing concentration (10 μM to 100 μM).

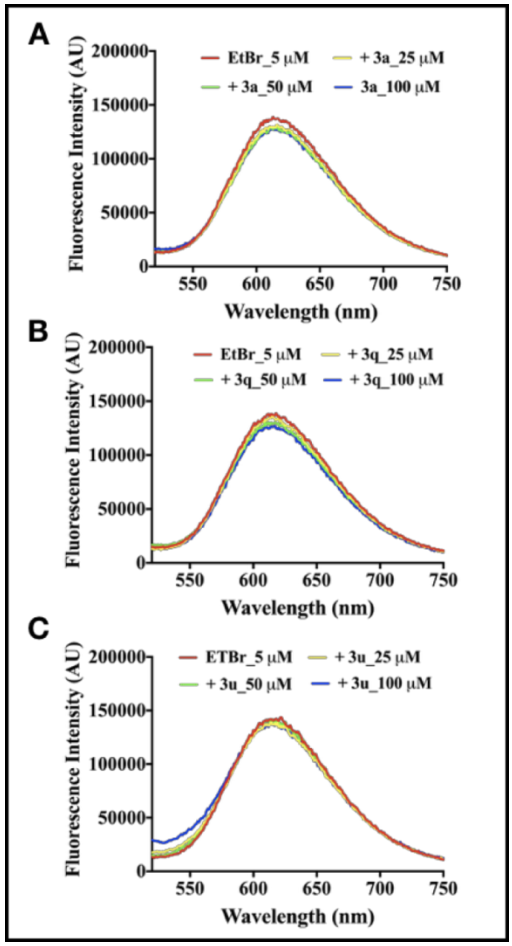


**Supporting Figure S11:** EtBr fluorescence quenching studies for compounds (A) **3a**, (B) **3q** and (C) **3u** in the presence of EtBr only in buffer (10 mM Na-P pH 7, 10 mM NaCl and 1 % DMSO)

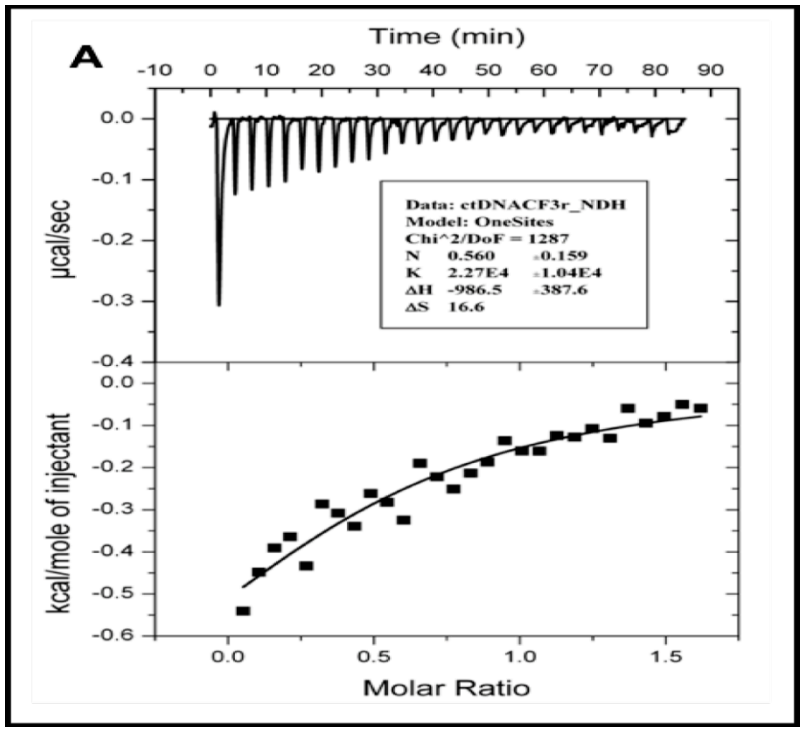
A
Time (min)
µcal/sec
kcal/mole of injectant
Molar Ratio
Data: ctDNACF3r_NDH
Model: OneSites
Chi^2/DoF = 1287
N 0.560 ±0.159
K 2.27E4 ±1.04E4
ΔH -986.5 ±387.6
ΔS 16.6

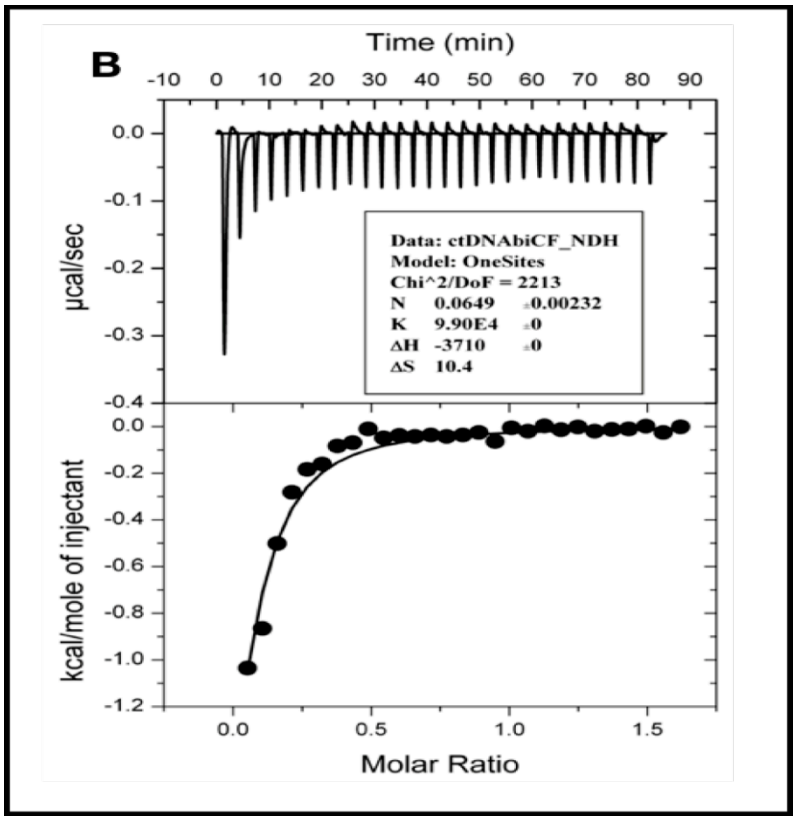
B
Time (min)
µcal/sec
kcal/mole of injectant
Molar Ratio
Data: ctDNAbiCF_NDH
Model: OneSites
Chi^2/DoF = 2213
N 0.0649 ±0.00232
K 9.90E4 ±0
ΔH -3710 ±0
ΔS 10.4

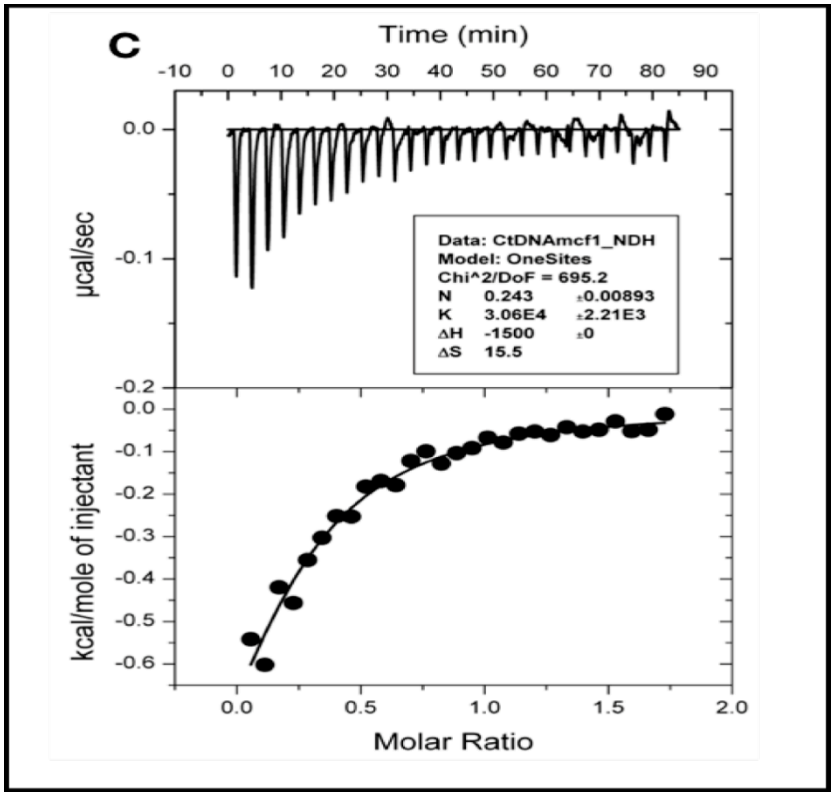


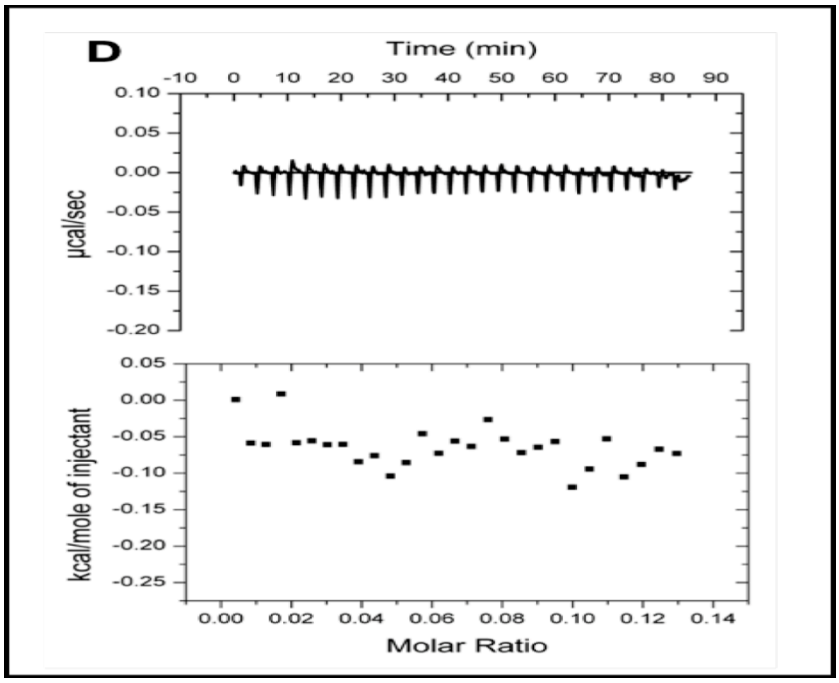


**Supporting Figure S12:** Isothermal titration calorimetric analysis of CT-DNA with (A) **3a**, (B) **3u**, (C) **3q** and (D) Buffer correction. Plots were drawn using Origin 7 software.[5]

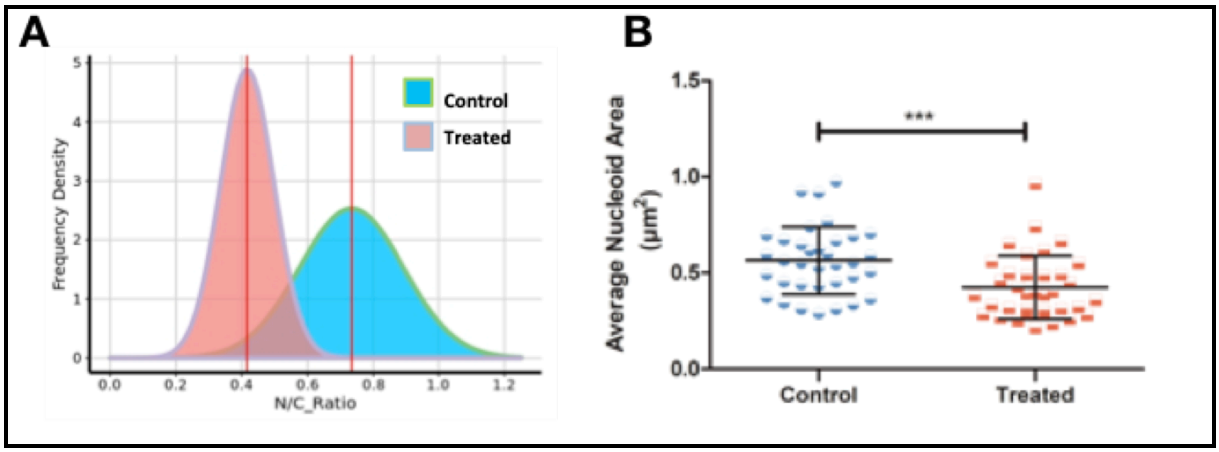


**Supporting Figure S13:** (A) Frequency density plot shows significantly different distribution for untreated and treated *S. aureus* cells with **3a** (control mean N/C = 0.73, treated mean N/C = 0.41). (B) Average nucleoid area also shows significant reduction in treated (0.423) S. *aureus* cells compared to control (0.56). (n=35).

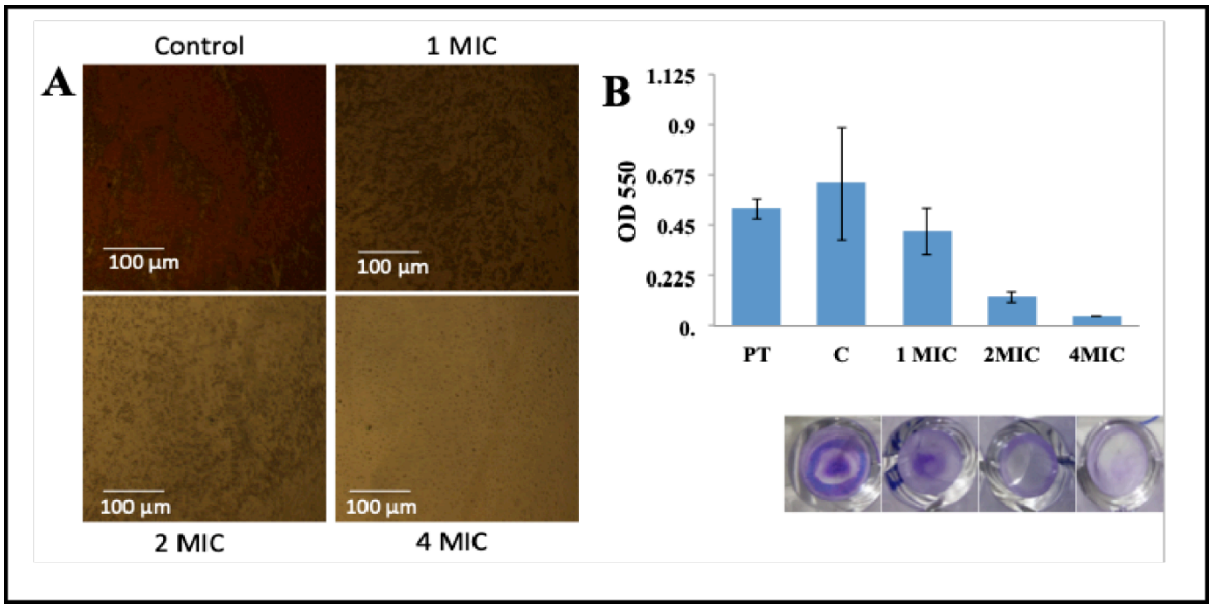


**Supporting Figure S14:** Disruption of preformed biofilm of *S. epidermidis* by **3a**. (A) Visualization of compound **3a** treated (1, 2, 4 MIC) or untreated *S. epidermidis* biofilm under light microscope at 20×. (B) Quantification and visualization of biofilm formation in bacteria using crystal violet stain.[6]

**Supporting Table 1:** Comparison Table of our synthetic derivatives with already available analogues.

| Sl. No. | Synthetic compounds/natural products | MIC (µg/mL) | | | |
|---|---|---|---|---|---|
| | | Gram positive bacteria | | Gram negative bacteria | |
| | | *S. aureus* | *S. epidermidis* | *E. coli* | *P. aeruginosa* |
| **1.** | **3a** | 1.79 | 2.24 | 3.36 | 6.73 |
| **2.** | **3b** | 3.78 | 3.78 | 3.78 | >10.07 |
| **3.** | **3c** | 3.47 | 3.47 | 2.31 | >9.24 |
| **4.** | **3f** | 3.03 | 4.32 | 4.32 | 10.80 |
| **5.** | **3h** | 3.45 | 3.45 | 4.59 | >11.48 |
| **6.** | **3m** | 3.36 | 2.24 | >22.42 | >22.42 |
| **7.** | **3q** | 0.89 | 0.89 | >8.96 | >6.72 |
| **8.** | **3s** | 1.69 | 0.96 | 7.24 | >7.24 |
| **9.** | **3t** | 0.93 | 1.63 | >9.33 | >6.99 |
| **10.** | **3u** | 1.03 | 0.52 | >7.75 | >7.75 |
| **11.** | 3-(5-Hexyl-3-phenylimidazo[1,5-a]quinoxalin-4-on-1-yl)-1-nonylpyridinium iodide.[7] | 0.78 | —— | >500 | >500 |
| **12.** | 2,3-Bis(bromomethyl)-6-(trifluoromethyl)quinoxaline.[8] | 12.5 | —— | >100 | >100 |
| **13.** | N-(2,3-di(furan-2-yl)quinoxalin-6-yl)-4-Nitrobenzenesulfonamide.[9] | 15 | —— | 25 | 30 |
| **14.** | Choles-5-en-3[thiazolo [4,5-b] quinoxaline-2-ylhydrazone.[1] | 0.78 | —— | 0.39 | —— |
| **15.** | 4-tert-Butyl-3-hydroxy-1,4-dihydrobenzo[g]quinoxaline-5,10-dione.[11] | 12.5 | —— | 12.5 | 12.5 |
| **16.** | Echinomycin (quinomycin A).[1] | 0.03125 | —— | 25 | >100 |
| **17.** | Triostin A.[1] | 0.625 | —— | >100 | >100 |

**REFERENCE:**

1. Cornish, A.; Fox, K. R.; Waring, M. J. Preparation and DNA-binding properties of substituted triostin antibiotics. *Antimicrob. Agents Chemother.* **1983**, *23*, 221-231.

2. Zhao, Y., Tian, Y., Cui, Y., Liu, W., Ma, W., Jiang, X. Small molecule-capped gold nanoparticles as potent antibacterial agents that target gram-negative bacteria. *J. Am. Chem. Soc*. **2010**, *132*, 12349–12356.

3. Niu, Y.; Wang, M.; Cao, Y.; Nimmagadda, A.; Hu, J.; Wu, Y.; Cai, J.; Ye, X. Rational design of dimeric lysine N-alkylamides as potent and broad-spectrum antibacterial agents. *J. Med. Chem.* **2018**, *61*, 2865−2874.

4. Mahata, T.; Kanungo, A.; Ganguly, S.; Modugula, E. K.; Choudhury, S.; Pal, S. K.; Basu, G.; Dutta, S. The benzyl moiety in a quinoxaline‐based scaffold acts as a DNA intercalation switch. *Angew. Chem. Int. Ed.* **2016**, *128*, 7864-7867.

5. Kwasny, S. M.; Opperman, T. J. Static biofilm cultures of gram-positive pathogens grown in a microtiter format used for anti-biofilm drug discovery. *Curr. prot. pharmacol.* **2010**, *50*, 13A.8.1-13A.8.23.

6. Buurma, N. J.; Haq, I. Advances in the analysis of isothermal titration calorimetry data for ligand–DNA interactions. *Methods.* **2007**, *42*, 162-172.

7. Kalinin, A. A.; Voloshina, A. D.; Kulik, N. V.; Zobov, V. V.; Mamedov, V. A. Antimicrobial activity of imidazo[1,5-a]quinoxaline derivatives with pyridinium moiety. *Eur. J. Med. Chem*. **2013**, *66*, 345-354.

8. Ishikawa, H.; Sugiyama, T.; Kurita, K.; Yokoyama, A. Synthesis and antimicrobial activity of 2,3-bis(bromomethyl)quinoxaline derivatives. *Bioorg. Chem*. **2012**, *41*, 1-5.

9. Kamal, A.; Babu, K. S.; Faazil, S.; Hussaini, S. A.; Shaik, A. B. L-Proline mediated synthesis of quinoxalines; evaluation of cytotoxic and antimicrobial activity. *RSC Adv*. **2014**, *4*, 46369-46377.

10. Khan, S. A. Synthesis, characterization and *in vitro* antibacterial activity of new steroidal 5-en-3-oxazolo and thiazoloquinoxaline. *Eur. J. Med. Chem*. **2008**, *43*, 2040- 2044.

11. Tandon, V. K.; Yadav, D. B.; Maurya, H. K.; Chaturvedi, A. K.; Shukla, P. K. Design, synthesis, and biological evaluation of 1,2,3-trisubstituted-1,4-dihydrobenzo[*g*]quinoxaline-5,10-diones and related compounds as antifungal and antibacterial agents. *Bioorg. Med. Chem*. **2006**, *14*, 6120- 6126.

---